

# Surface characterization of nanoparticle coated paperboard

M. Stepien\*<sup>†</sup>, J. J. Saarinen\*, H. Teisala\*\*, M. Tuominen\*\*, M. Aromaa\*\*\*,  
G. Chinga Carrasco<sup>b</sup>, J. Kuusipalo\*\*\*, J. M. Mäkelä\*\*\* and M. Toivakka

\* Paper Coating and Converting, Abo Akademi University, Åbo, Finland, <sup>†</sup>milena.stepien@abo.fi

\*\* Paper Converting and Packaging Technology, Tampere Univ. of Technology, Tampere, Finland

\*\*\* Aerosol Physics Laboratory, Tampere University of Technology, Tampere, Finland

<sup>b</sup>Paper and Fibre Research Institute AS (PFI), Trondheim, Norway

## ABSTRACT

Both surface topographical and chemical composition of nanoparticle coated paperboard was characterized to explain observed differences in surface wettability. TiO<sub>2</sub> particles induce superhydrophobicity with water contact angle (CA) of 161° whereas SiO<sub>2</sub> particles result in superhydrophilicity with 23° water CA. The nanoparticles were generated by the liquid flame spray (LFS) process. The morphological characterization of reference paperboard and nanocoated samples was performed using FESEM and AFM. Both XPS and CA measurements were used to evaluate chemical composition before and after nanoparticle deposition. Our results show that the LFS process can be used to create either hydrophobic or hydrophilic paperboard depending on the type of nanoparticles used for coating. The wettability differences were contributed to the attributed effect of surface chemistry and topography.

**Keywords:** liquid flame spray process, surface analysis, nanocoatings, paperboard

## 1 INTRODUCTION

Development of new products involves proper choice of materials and methods, but also a good understanding of the substrate properties. Paperboard belongs to a group of products, which has the advantage of being renewable, commonly available, and cost-efficient with excellent potential for use as the base substrate in numerous applications. In addition, it is possible to adjust the properties for the intended end-use simply by choosing appropriate manufacturing conditions [1], [2]. At the same time, it is necessary to have a good understanding of the substrate properties as well as the manufacturing methods. Therefore, the development procedure requires support from analytical tools and material characterization. This is especially important at the interfacial regions.

It is well known that wettability is important both from fundamental and applied points of view. Interactions at the interfaces with different liquids affect the bond formation, reactivity, and final properties of the substrate [3]. Likewise, these terms are also crucial for many industrial applications, for example, in paper

coating, printing, extrusion, or lamination processes [4]. In the past we have investigated wetting properties of paperboard modified by nanoparticle deposition during the liquid flame spray (LFS) process [5]. The LFS process utilizes a high temperature and high velocity flame, which is fixed above a moving paperboard web. For nanoparticle deposition, an organometallic feedstock is dissolved in liquid, and injected into the flame. The oxygen-hydrogen flame evaporates the liquid solvent, and creates molecules, which can react chemically or decompose thermally. As a result of nucleation, nanoparticles of the final material can be deposited on the surface of paperboard. For more detailed information of the sample preparation and LFS process, see Refs. [5], [1], [7], [8]. The process was successfully used for adjusting the paperboard function, and is an alternative for other existing methods such as plasma deposition [6] used for surface treatment as a one-step, on-line coating process.

Here we focus on the surface characterization of paperboard, whose wetting properties were changed by the deposition of nanoparticles. The LFS process was used with two different liquid precursors for titanium and silicon oxide nanodeposition. First, a field emission scanning electron microscopy (FESEM) in different modes and atomic force microscopy (AFM) were applied for performing a comprehensive surface analysis. Secondly, X-ray photoelectron spectroscopy (XPS) was used to identify the chemical state of those nanodeposits. Next, contact angle (CA) measurements as well as XPS were used to collect information about the induced superhydrophobic and superhydrophilic behavior of the paperboard. The purpose of this work is to correlate the changes in wetting properties of paperboard with nanosized TiO<sub>2</sub> and SiO<sub>2</sub> coatings produced by the LFS process.

## 2 EXPERIMENTAL

Two different nanocoatings were deposited on a commercially available double pigment coated paperboard (grammage 200 g/m<sup>2</sup>, Natura, Stora Enso, Skoghall, Sweden) using the LFS process. Nanoparticle generation was performed in a continuous roll-to-roll process at ambient conditions with a constant web speed of 50 m/min. Figure 1 presents a schematic set-up of the pro-

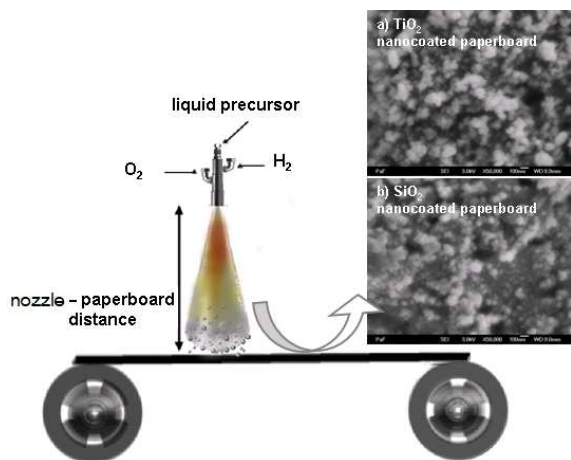


Figure 1: The liquid flame spray set-up.

cess for deposition of  $\text{TiO}_2$  and  $\text{SiO}_2$  nanoparticles. In this study, the liquid precursors used for nanoparticle coatings were dissolved in isopropanol (IPA): titanium (IV) isopropoxide (TTIP) was used for  $\text{TiO}_2$  coatings and tetraethylorthosilicate (TEOS) for  $\text{SiO}_2$  coatings. Metal ion concentration of 50.0 mg/ml was fed with a rate of 32.0 ml/min into a nozzle that was fixed at 15 cm distance from the substrate. Subfigures 1 a) and b) display SEM images of  $\text{TiO}_2$  and  $\text{SiO}_2$  nanocoated surfaces.

A detailed structural analysis of the nanocoated surfaces was performed with several microscopy techniques at different scales. Images were collected with a commercial scanning electron microscopy (SEM) (Jeol JSM-6335F) and analytical variable pressure scanning electron microscope (VP FE-SEM) (Hitachi SU 6600). All samples were gold or carbon coated to obtain conductivity before imaging. In addition, various complementary VP FE-SEM modes were applied for performing a comprehensive surface analysis. Secondary electron imaging (SEI) mode was used for surface structural analysis at several magnifications (5000-100 000x), SEI resolution of 3.0 nm (WD = 4mm, Mag: 80kX). Backscatter electron imaging (BEI) mode was applied for cross-sectional analysis of the coating structure, BEI resolution 3.5 nm (WD = 8mm, Mag: 80kX, 10Pa). BEI made it possible to explore the cross-sectional characteristic details. The structural assessment was complemented with an Energy-Dispersive Spectroscopy (EDS) analysis, which gives an opportunity to reveal the surface element composition. Atomic force microscope (AFM) was a commercial NT-MDT NTEGRA Prima (Moscow, Russia) instrument. Uncoated rectangular silicon cantilevers (Europe MicroMasch, Estonia) with a resonance frequency of 212 – 220 kHz were used for imaging. All images (1024 × 1024 pixels) were captured using the tapping mode in ambient conditions (RT 24°C ± 1°C

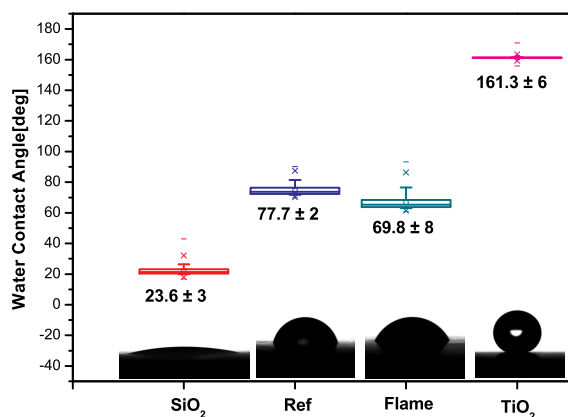


Figure 2: A water contact angle of reference double pigment coated paperboard (blue), flame treated reference paperboard (green),  $\text{SiO}_2$  (red) and  $\text{TiO}_2$  (pink) coated samples. A box chart represents values of water contact angle with standard deviation from three different parallel measurements. The subfigures under the boxes correspond to the values of water contact angle taken after 2 seconds of measurement for each sample.

and RH 38 ± 5 %). For imaging damping ratio ( $A_{sp}/A_0$ ), where  $A_{sp}$  is a set-point amplitude and  $A_0$  is free amplitude and line frequency, was set to 0.5 – 0.6 and 0.36 – 0.97 Hz, respectively.

Contact angle (CA) measurements were performed by a commercial contact angle goniometer KSV CAM 200 (KSV Instruments Ltd., Finland). The tests were performed by dispensing purified (Milli-Q filtration unit, Millipore, U.S.A., resistivity 18.2MΩ) water droplets with a volume of approximately 2.0 μl. The results are given as an average of at least three determinations for each sample measured in air at ambient conditions (room temperature (RT) 23°C ± 1°C and relative humidity (RH) 30 ± 5 %).

X-ray photoelectron spectroscopy spectra of reference paperboard and nanocoated sample surfaces were acquired using PHI Quantum 2000 X-ray photoelectron spectrometer (Physical electronics instruments, USA) equipped with a monochromatic  $\text{AlK}\alpha$  X-ray source operated at 25 W. The samples were irradiated with monoenergetic X-rays for 10 minutes with a pass energy of 184 eV for survey analysis causing photoelectrons to be emitted from the sample surface with an emission current of 2 mA. At least three different areas of approximately 100 μm in diameter were studied for each sample. For high resolution carbon C 1s peak, oxygen O 1s peak, silicon Si 2p peak, and titanium Ti 2p peak spectra were recorded with the pass energy of 29.35 eV after 10 minutes of measurement. A mixed Gaussian-Lorentzian character and Shirley background were used for curve fitting of high resolution peaks. The binding energy of spectra was first related to C1 (C-C, C-H) peak

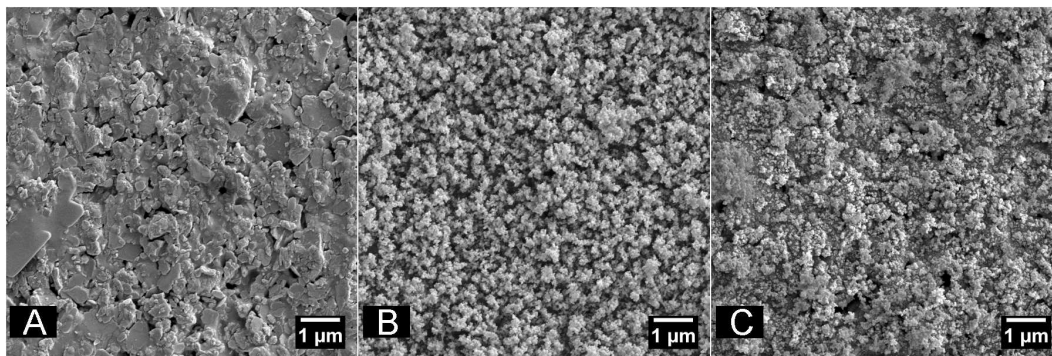


Figure 3: FESEM analysis. (A) Reference paperboard. (B) Surface after deposition of  $\text{TiO}_2$  nanoparticles. (C) Surface after deposition of  $\text{SiO}_2$  nanoparticles.

and the following relative chemical shifts were employed for the relevant groups:  $1.7 \pm 0.2$  eV for C2 (C-O, C-OR),  $3.1 \pm 0.3$  for C3 (O-C-O, C=O),  $4.6 \pm 0.3$  for C4 (O=C-O) and C5 with 5 eV chemical shift for carbonate group [9], [10].

### 3 RESULTS

Figure 2 displays water CA values. The highest CA of  $161^\circ$  was obtained for  $\text{TiO}_2$  coating and the lowest of  $24^\circ$  for  $\text{SiO}_2$ , while the reference paperboard and flame treated paperboard gave  $78^\circ$  and  $70^\circ$ , respectively. These results indicate that the LFS process can be used as a simple method to create either hydrophobic or hydrophilic paperboard simply by choosing different metal ions in a liquid precursor. The subfigures display images of water droplets taken after 2 seconds of measurement.

Figure 3 display the FE-SEM images of reference paperboard (A), surface after deposition of  $\text{TiO}_2$  nanoparticles (B), and surface after deposition of  $\text{SiO}_2$  nanoparticles (C). The FE-SEM SEI mode images reveal that the paperboard surface is fully covered by the nanoparticles, which form a dense, complex coating structure containing a number of summits and voids. Based on the collected images it was possible to observe that sizes of deposited nanoparticles are similar and range between 25-60 nm. Fig.4 A, and B show cross sectional images of  $\text{TiO}_2$  nanocoated surface, acquired in BEI mode. Based on these images and the EDS spectra collected from the corresponding areas (Fig. 4 C), it was confirmed that the deposited layer is composed of  $\text{TiO}_2$  nanoparticles with thickness less than 100 nm.

In order to quantify the surface texture, the surface roughness parameters were measured using atomic force microscopy, as reported by Stepien *et al.* [5]. Three roughness parameters were defined: the root mean square (RMS) roughness  $S_q$ , the surface area ratio  $S_{dr}$ , and density of summits  $S_{ds}$ . For  $\text{TiO}_2$  nanocoated sample the observed values were  $S_q = 94.3$  nm,  $S_{dr} = 111.4\%$ , and

$S_{ds} = 472.2 \mu\text{m}^{-2}$  whereas the corresponding parameters for  $\text{SiO}_2$  nanocoated surface were  $S_q = 86$  nm,  $S_{dr} = 44.3\%$ , and  $S_{ds} = 86.1 \mu\text{m}^{-2}$ . The RMS roughness of both  $\text{TiO}_2$  and  $\text{SiO}_2$  coatings increased compared to the reference sample. Differences in the nanoparticle coatings were observed in the  $S_{dr}$  and  $S_{ds}$  parameters. The results showed that the surface area of  $\text{TiO}_2$  sample is much larger than that of the  $\text{SiO}_2$  coated sample. The number of local maxima  $S_{dr}$  gives additional supporting information as there is a clear difference in  $\text{TiO}_2$  sample (472.0) compared to  $\text{SiO}_2$  sample (86.1) and the reference paperboard (99.6).

Surface chemical composition of paperboard samples was investigated by X-ray photoelectron spectroscopy (XPS). The low and high resolution XPS spectra showed changes in the surface chemistry before and after the LFS process. From the XPS results obtained for Reference, Flame,  $\text{SiO}_2$ , and  $\text{TiO}_2$  nanocoated samples the amount of carbon and oxygen was compared in Fig. 5. In addition, the high-resolution decomposition of a C1s peak was performed to calculate the ratios of C2 to C1 for each sample. The low resolution XPS spectra showed that the LFS process increased the ratio of O to C of the surface. Results for the  $\text{SiO}_2$  sample show the greatest increase in oxidation level as well as C2 carbon related groups. On the other hand, for  $\text{TiO}_2$  nanocoated sample both ratios are on the same level or just slightly higher than for the reference or flame sample. The increased value of O to C ratio is connected to the value of C1 peak from the second ratio. Since C1 peak represents the hydrocarbon type of bonds, and C2 carbon-oxygen type of bonds, we conclude that  $\text{SiO}_2$  nanocoated sample has also the highest relative amount of hydroxyl groups on the surface. On the other hand, carbon C1 is on much higher level for  $\text{TiO}_2$  than  $\text{SiO}_2$  nanocoated sample. These findings may be related to the replacement of hydroxyl groups by the aliphatic chains on the surface of  $\text{TiO}_2$  nanoparticles of the superhydrophobic sample.

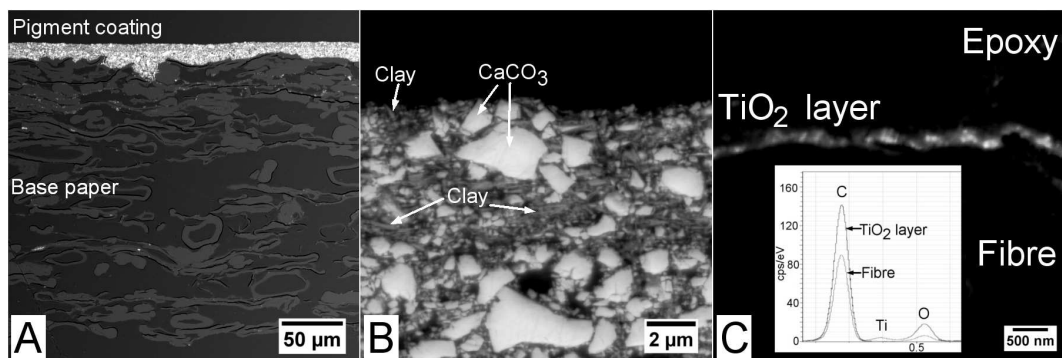


Figure 4: BEI/EDS analysis of cross-sectional structure after TiO<sub>2</sub> nanoparticle deposition. (A) Cross sectional BEI mode image of coated board. (B) Coating layer cross-sectional structure. (C) The corresponding EDS spectrum confirms that the deposited layer consists of TiO<sub>2</sub>.

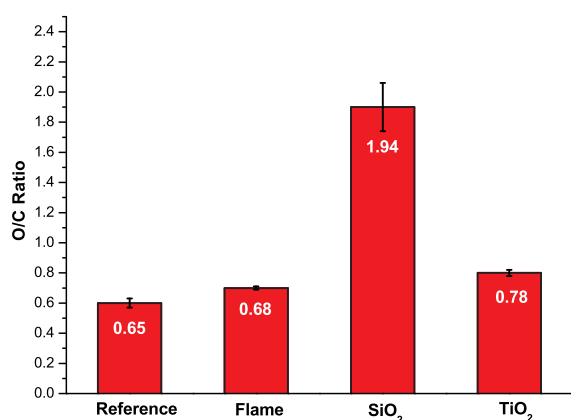


Figure 5: The ratios of O to C obtained by low-resolution XPS for reference double pigment coated paperboard (Reference), flame treated reference paperboard (Flame), SiO<sub>2</sub> and TiO<sub>2</sub> coated samples.

## 4 CONCLUSIONS

We have presented a detailed surface characterization of paperboard surface before and after deposition of nanoparticles. The LFS process can be used to create nanoparticles with different surface wetting properties depending on the type of particles used for coating. The TiO<sub>2</sub> nanocoating on paperboard creates a highly hydrophobic surface, whereas SiO<sub>2</sub> nanocoating creates a highly hydrophilic one. The wettability differences are related to the surface topography and surface chemistry of paperboard and the created nanoparticles. Detailed FE-SEM and AFM analysis show that both nanocoatings completely cover the surface and increase the roughness, compared to the reference sample. The calculated roughness values are higher for TiO<sub>2</sub> coated sample than for SiO<sub>2</sub>. The XPS results show that in the SiO<sub>2</sub> sample oxidation level is high, while it is low in the TiO<sub>2</sub> sample. On the other hand, there is much

more carbon C1 in the TiO<sub>2</sub> nanocoated sample than in the SiO<sub>2</sub> nanocoated sample. These findings may be related to the replacement of hydroxyl groups by aliphatic chains in the superhydrophobic TiO<sub>2</sub> coated sample. At the same time, small material amounts (20–50 mg/m<sup>2</sup>), and a relatively simple setup and continuous roll-to-roll process flow allows a scale-up for industrial use, which makes it possible to coat large volumes at high line speeds.

## Acknowledgments

This work was funded by the Finnish Funding Agency for Technology and Innovation (Tekes) under "Liquid flame spray nanocoating for flexible roll-to-roll web materials" – project (grant no. 40078/08 and 40095/11)

## REFERENCES

- [1] H. Teisala *et al.* Surf. Coat. Technol, 205, 436–445, (2010).
- [2] J. M. Mäkelä *et al.* Aerosol Sci. Technol., 45, 817–827, (2011).
- [3] A. Chattopadhyay *et al.* Surf. Coat. Technol, 204, 410–417, (2009).
- [4] J. Berg, Marcel Dekker, 2–11, (1993).
- [5] M. Stepien *et al.* Appl. Surf. Sci., 257, 1911–1917, (2011).
- [6] M. Pykönen *et al.* Surf. Coat. Technol., 202, 3777–3786, (2008).
- [7] J. Tikkanen *et al.* Surf. Coat. Technol., 90, 210–216, (1997).
- [8] J. M. Mäkelä *et al.* J. Mater. Sci., 39, 2783–2788, (2004).
- [9] G. Ström *et al.* Nordic Pulp Paper Res. J., 1, 105–112, (1993).
- [10] J. Moulder *et al.* Perkin-Elmer Corp., (1992).